Physical and electrochemical contributions to the cell voltage in the thin-layer electrochemical deposition of copper at constant current

John R. de Bruyn
Department of Physics and Physical Oceanography, Memorial University of Newfoundland, St. John's, Newfoundland, Canada A1B 3X7
(Received 9 May 1997)

Many different processes affect the voltage across an electrochemical cell during electrochemical deposition in a thin-layer geometry. I report detailed measurements of the cell voltage as a function of time in experiments on the deposition of ramified copper aggregates from thin layers of $CuSO_4$ electrolyte. Experiments were performed for a range of electrolyte concentrations and cell currents. The effects of various physical phenomena, including hydrodynamic convection, instability of the growing electrodeposit, and local variations in the growth rate of the aggregate are identified and studied, as are the contributions due to electrochemical phenomena. [S1063-651X(97)11609-9]

PACS number(s): 81.15.Pq, 47.20.Bp

I. INTRODUCTION

The growth of branched metal aggregates by electrochemical deposition (ECD) in quasi-two-dimensional geometries is an interesting and complex example of nonequilibrium growth [1,2]. In a typical experiment, a thin layer of unsupported binary electrolyte is confined between two transparent plates. Thin metal foils or wires are used as electrodes, with the distance between the electrodes much larger than the cell thickness. When a current is passed through the cell, metal cations come out of solution at the cathode and grow into a branched aggregate [3,4]. A variety of different growth morphologies have been observed, depending on the experimental conditions [3–6]. This system has been studied extensively, with much of the interest centering on the end product, that is, on the nature and morphology of the deposited aggregate [3–7]. More recently, considerable progress has been made towards understanding the interplay among the various electrochemical and physical processes that play a role in these experiments [8–24]. Ions drift in the applied electric field and electrochemical reactions occur at both cathode and anode. These reactions lead to spatial variations in the concentration of ions near both electrodes, which drive diffusive ion transport there and also lead to buoyancy-driven convective flows [19–24]. Convection can also be driven by electric fields acting on regions of space charge near the tips of the branched aggregate [12–14,21,23]. Thus ions are transported in the cell by a complicated combination of migration, diffusion, and convection. As well, changes with time in the ion concentrations at the electrodes can trigger new electrochemical reactions or lead to time dependence in the electrode processes [25–27]. All of these factors affect the deposition of metal ions at the cathode, and the presence of the metal aggregate itself can in turn affect the processes taking place in the cell.

In this paper I report on a series of experiments on the electrochemical deposition of Cu aggregates from aqueous solutions of $CuSO_4$. The experiments were performed at constant applied current, and the cell voltage V was recorded as a function of time t. The measurements of $V(t)$ were supplemented by video recordings of the growth of the aggregate. Electrochemical cells are strongly non-Ohmic, and the behavior of $V(t)$ is quite complex. The main results presented in this paper concern the interpretation of features in the $V(t)$ data in terms of the physical and electrochemical processes described briefly above, and, where possible, their relationship to corresponding features in the growing aggregate.

The cell voltage is a global measure of what is happening in the ECD cell, and without additional measurements it is impossible to differentiate between anodic and cathodic contributions to $V(t)$. The measurements reported here are for the most part at early times, from before to shortly after the appearance and development of branched growth on the cathode. In the same regime, as discussed below, the only things expected to happen at the anode are the gradual buildup of SO_4^{2-} concentration and the subsequent development of convection there. In this paper we make the assumption, which is consistent with the results of previous studies in which the cathode potential was measured relative to a reference electrode [20,28], that most of the interesting changes in $V(t)$ are due to cathodic processes [29].

In the remainder of this section, the processes that contribute to $V(t)$ are outlined in more detail. I then briefly review some of the recent research on this system, with emphasis on work involving measurements of the cell voltage. The experimental details are described in Sec. II, and the results presented in Sec. III. Section IV is a discussion, and the conclusions drawn from this work are summarized in Sec. V.

When the current through the cell is turned on, Cu^{2+} cations start to drift towards the cathode and SO_4^{2-} anions drift towards the anode. A potential drop also develops across double layers at the electrode surfaces. In the absence of rough growth on the electrodes, charging of the double layers takes a few ms, and is fast on the time scale of the experiments. When the cations reach the cathode they are quickly reduced and plate out there as metallic copper. This results in a region very close to the cathode in which the ion concentration is lower than in the bulk [18–20]. As the concentration gradient there becomes stronger, diffusive transport across the depletion region becomes important.

If the current is entirely diffusive, then for constant current density i, the concentration $c(x,t)$ is given by [30]

$$c(x,t)=c_0-\frac{2i}{nF}\left(\frac{t}{\pi D}\right)^{1/2}\exp^{(x^2/4Dt)}+\frac{ix}{nFD}\mathrm{erfc}(x/\sqrt{4Dt}), \tag{1}$$

where the cathode is at $x=0$ and $c(x,0)=c(\infty,t)=c_0$. Here n is the ion charge, F the Faraday constant, and D the diffusion constant. The concentration at the cathode $c(0,t)$ decreases with time, eventually reaching zero at the time

$$t_s=\pi Dn^2F^2c_0^2/4i^2. \tag{2}$$

The time t_s is called the transition time, or the Sand's time. In the present case, migration and convective transport are also important and modify these results [15,18].

Since the conductivity of the electrolyte goes to zero as c_0 goes to zero, while the current remains constant, $V(t)$ must diverge at t_s. In practice the cell voltage increases, or more correctly, the potential of the cathode becomes more negative with respect to the anode, until a new process—for example, a new electrochemical reaction — takes over the job of providing ions to the electrode. The cell voltage then levels off at a new value. Further transition times, and further increases in the cell voltage, can occur as the reactants for each successive process become depleted. Measurements of $V(t)$ and t_s can be used to determine the properties of electrolytes [30], but the utility of this as an analytical technique is limited by the effects of convection, and also by the fact that when $V(t)$ changes, some of the current goes into charging the double layers, leading to deviations from Eq. (2), and a smearing out of the transition. This makes it difficult to determine t_s precisely. In the present work, we identify transition times with inflection points in $V(t)$, i.e., with the times at which dV/dt is a maximum.

The concentration gradient that develops at the cathode according to Eq. (1) leads to a density gradient, which in turn drives the development of a buoyancy-driven convection roll (a gravity current) near the cathode. At the anode the ion concentration increases, since SO_4^{2-} ions arriving there do not come out of solution, and so convection develops there as well. The development of buoyancy-driven convection in ECD and the effect of gravity currents on the growth of the aggregate have been studied by several groups [19–24]. Recently Huth *et al.* [23] have performed a detailed study of gravity currents at the electrodes, in which they measured convective flow velocities by tracking neutrally buoyant particles advected by the flow.

The diffusion-limited growth of a uniform metal aggregate is unstable to a variant of the well-known Mullins-Sekerka instability [8,31–34]. The concentration gradient near a small outward perturbation on the cathode will be enhanced, and so the diffusive transport of ions toward this perturbation will be higher than to flat regions nearby. As a result the perturbation will grow, leading to the development of rough growth. In our experiments the transport of cations becomes diffusion limited when the concentration of ions at the cathode becomes zero, so the onset of this instability can therefore be associated with the transition time t_s [18].

When a branched aggregate exists at the cathode, electroconvection can occur near the tips of the branches [12–14,21,23]. The electric field in the cell is highest there due to the shape of the tips and to the high resistance of the depletion zone adjacent to the aggregate. Regions of positive space charge also exist near the tips, due to the fact that the anions drift away from the cathode while the cations diffuse towards it. The field can interact with the space charge to drive convective flow, which takes the form of pairs of counterrotating vortices bracketing the branch tip [12–14,21,23,35]. This flow transports cations towards the tips and so affects the growth, and it is strong enough to cause substantial physical motion of the fine branches [36].

The resistance of the electrolyte in the cell leads to an Ohmic contribution to the cell voltage. This voltage decreases with time as the aggregate grows and short circuits the electrolyte behind its leading edge. It is straightforward to show that the Ohmic voltage drop across the cell $V_\Omega(t)$ is given by [9]

$$V_\Omega=\frac{Id}{\sigma A}-\mu\left(\frac{I}{\sigma A}\right)^2 t, \tag{3}$$

where I is the current through the cell, d the cell length, and A its cross-sectional area. σ is the conductivity of the electrolyte and μ the mobility of the anions. The linear decrease of V_Ω with time is due to the constant growth speed of the aggregate, which is in turn the same as the drift speed of the anions moving away from the cathode [9,22]. The rate of decrease depends on both I and the concentration c_0, since σ increases with c_0 [37].

Fleury *et al.* [11] measured the cell voltage as a function of time and identified three regimes: an initial increase in $V(t)$ before the first appearance of branched growth on the cathode, followed by a linear decrease as the aggregate grew, and finally a noisy regime that occurred when the aggregate was very close to the anode. They found the slope dV/dt in the linearly decreasing regime to be proportional to i^2, as predicted by Eq. (3). Fleury *et al.* [10,11] also observed a change in slope at the morphological transition known as the Hecker transition [10]. This transition is due to the arrival of a front of increased H^+ concentration from the anode [10,11,16], which also results in an increase in conductivity and so a change in slope. Another morphological transition, however, had no obvious signature in the $V(t)$ data [10]. Similar results were found in the ECD of zinc by Kuhn and Argoul [16], who also noted that the slope in the regime of linear decrease depended on the growth speed of the aggregate, with faster growth leading to a steeper decrease in $V(t)$, in agreement with Eq. (3).

Chassaing *et al.* [28] and Rosso *et al.* [20] made similar observations, noting an initial transient overshoot in the cell voltage followed by an increase compatible with Sand's behavior. Then came a further increase at a rate slower than predicted by Eq. (1), during which some ramified deposition became visible, then a kink in $V(t)$ after which the ramified aggregate grew more quickly, and finally a linear decrease in $V(t)$.

Argoul and Kuhn [27] also studied $V(t)$ curves during the thin layer ECD of zinc. They identified several regimes, beginning with a period of ''concentration polarization'' during

which $V(t)$ increased due to the decrease in $c(0,t)$. After the transition time they observed oscillations in $V(t)$ that they explained as being due to oscillations in the electrochemical reactions taking place at the cathode, involving the reduction of Zn^{2+} and H^+, the formation of a layer of $Zn(OH)_2$ on the electrode, and then the reduction of the $Zn(OH)_2$ to metallic zinc. They noted that in general an increase in cell voltage implied a slowing down of the growth of the aggregate. Chaotic variations in $V(t)$ have also been observed for this system [26].

Recently Argoul *et al.* [18] studied the electrodeposition of zinc at constant current. They used interferometry to study the development of concentration gradients near the electrodes, and compared their observations with the features observed in the cell voltage. A narrow region depleted in ions was rapidly established very close to the cathode. Although the resulting concentration gradients led to the development of buoyancy driven convection near the cathode, which contributed to ion transport, they found that close to the cathode the concentration $c(x,t)$ was reasonably well described by Eq. (1), although with an effective diffusion constant $D_{\rm eff}$ an order of magnitude larger than the expected value for $ZnSO_4$ solutions. At a time referred to by Argoul *et al.* as the ''microscopic Sand's time,'' the concentration at the cathode reached zero, V increased rapidly, and small-scale roughness became visible on the interface of the metal being deposited on the cathode. Oscillations in $V(t)$ also appeared. They also identified a ''macroscopic Sand's time,'' corresponding to the time at which large-scale roughness became visible at the cathode and to the maximum of $V(t)$.

II. EXPERIMENT

The experimental apparatus used in the present work was similar to that described previously [22,34]. The ECD cell consisted of two copper foil electrodes 5.1 cm long by 0.025 cm thick, separated by approximately 2.3 cm. These were sandwiched between two 5.1 cm square by 0.6 cm thick glass plates, which were then clamped together. Before each run, the electrodes were polished with fine emory paper. Both the electrodes and the glass plates were rinsed with water and then cleaned with acetone, which was allowed to evaporate. The space between the electrodes was filled with solutions of $CuSO_4$ in distilled deionized water [39]. A Keithley 220 programmable current source was used to provide constant cell currents. Over 80 runs were performed with electrolyte concentrations c_0 in the range $0.02<c_0<0.5$ mol/liter and currents in the range $0.06<I<10$ mA, as shown in Fig. 1. For a given concentration, at high currents the process was very fast and accompanied by the formation of numerous hydrogen bubbles. At low currents, on the other hand, the process was very slow, and after about an hour air would begin to invade the cell from the sides, which were not sealed. These considerations limited the range of currents studied in this work.

The cell voltage $V(t)$ was recorded with a Keithley 196 digital multimeter at intervals of from 0.5 to 5 s, depending on experimental conditions. The data were transmitted via an IEEE-488 bus to a personal computer for later analysis. Experiments were performed at room temperature, which was not specially controlled.

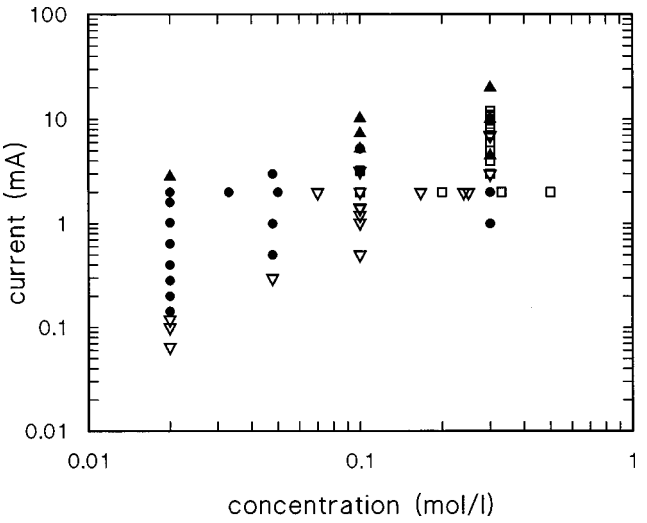

FIG. 1. Diagram showing the currents and concentrations of the experimental runs. The different symbols indicate which transitions were observed for each run, as discussed in the text. Upward-pointing triangles: only the transition at t_1 was observed; circles: t_1 and t_2; squares: t_0 and t_1; downward-pointing triangles: t_0, t_1, and t_2.

The cell was mounted on a rigid aluminum frame and was illuminated from below by a white light source made diffuse by passing it through an opal glass plate. The cell was imaged from above with a charge-coupled device video camera and a Navitar MagnaZoom video microscope, and the growth of the copper aggregate at the cathode was recorded on video tape. Individual images of the aggregate were also captured and digitized every few seconds by a frame grabber in the personal computer. The field of view was from 5 to 15 mm in the direction parallel to the electrodes, depending on the microscope magnification used, corresponding to a spatial resolution in the digitized images of between 8 and 23 μm/pixel.

III. RESULTS

A. Overview

Figure 2(a) shows a typical plot of the cell voltage V as a function of time t, measured in a run with $I=2.00$ mA and $c_0=0.07$ mol/liter. If we make the assumption that the anode potential remains fixed during the run [29], then changes in $V(t)$ result from changes in the cathode potential, with an increase in $V(t)$ corresponding to the cathode potential becoming more negative. Figure 2(b) is a plot of dV/dt for the same run. When the current through the cell is turned on at $t=0$, the cell voltage rises essentially immediately to a certain value, then drops back to a slightly lower voltage over a few seconds. $V(t)$ then passes through a minimum before increasing rapidly in one or more steps. These steps indicate transitions in the electrode processes, as discussed in the Introduction, and are accompanied by corresponding peaks in dV/dt. Two prominent peaks are visible in Fig. 2(b), as well as a weak shoulder on the low-t side of the larger peak. These three features appear in other runs, although their rela-

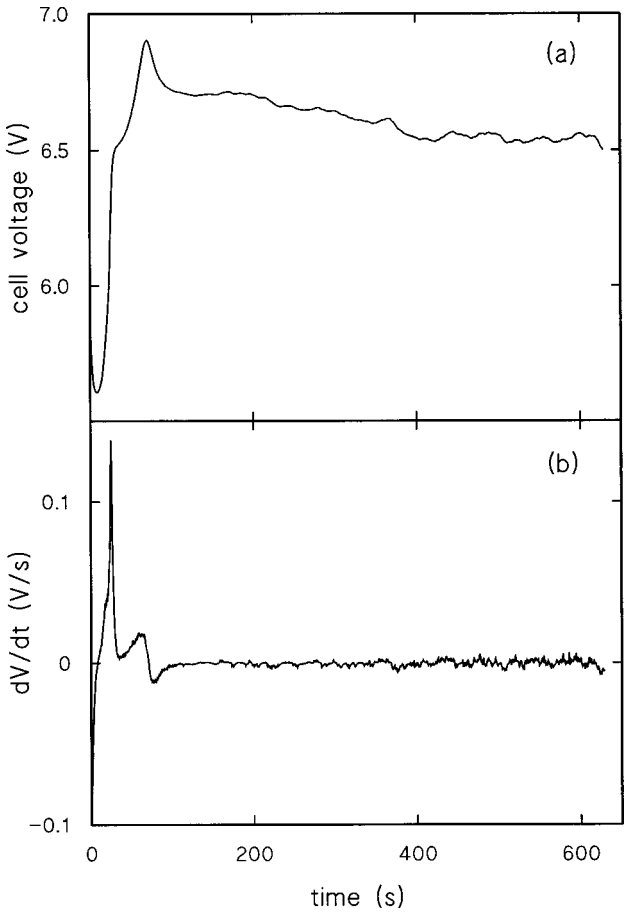

FIG. 2. (a) The cell voltage $V(t)$ for a run with $c_0=0.07$ mol/liter and $I=2.00$ mA. (b) dV/dt for the same run.

tive strengths vary and not all of them are visible in all runs. In Fig. 2, the largest peak in dV/dt is associated with the appearance of rough growth on the cathode. We label the time at which this peak occurs as t_1 and the corresponding cell voltage as V_1. The shoulder before the main peak occurs at a time designated t_0 and a voltage V_0. At higher concentrations this feature is much stronger, and is associated in many runs with the appearance of oscillations in $V(t)$. An example is shown in Fig. 3, in which two sets of oscillations occur, one starting at $t_0=87$ s, and one starting later at $t\approx 150$ s. A detailed study of these oscillations, which may be similar in origin to those observed in the ECD of zinc by Argoul and Kuhn [27], will be published elsewhere. Finally, we label the time and voltage of the peak in dV/dt that occurs after the main peak as t_2 and V_2. This feature does not seem to be associated with any obvious changes in the growth or morphology of the aggregate. Following the appearance of some or all of these features, $V(t)$ reaches a maximum value $V_{\max}$, after which the cell voltage eventually decreases approximately linearly, but with large fluctuations.

Figure 1 shows the currents and concentrations at which various combinations of these three features were observed. At the highest currents, only a single peak was seen in dV/dt. As the current was decreased at low concentrations, the t_2 peak appeared after the main peak, while at higher concentrations the t_0 peak became visible before t_1. In the slowest runs at low current, all three features were observed.

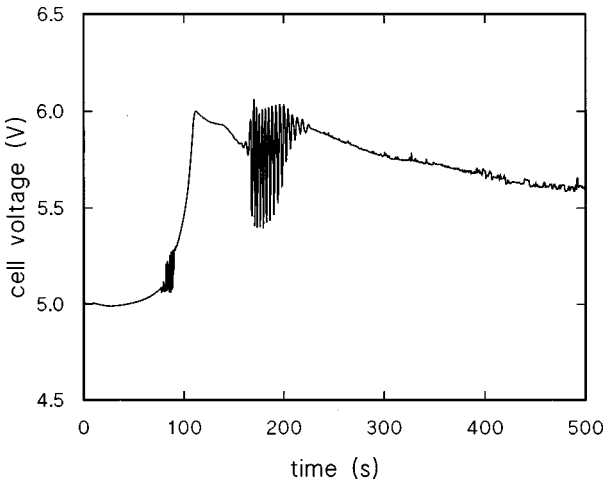

FIG. 3. (a) $V(t)$ for a run with $c_0=0.3$ mol/liter and $I=5.00$ mA. Oscillations occur both before and after the main transition.

In Sec. III B results concerning the transition times and the potentials at which the transitions occurred are presented. Section III C involves the results of measurements of the transient decrease in $V(t)$, which occurs at the start of the runs, and Sec. III D concerns the linear decrease at later times.

B. Transitions

In what follows we measure voltages relative to $V_{\min}$, the minimum value of $V(t)$ following the initial transient, and define $\Delta V=V-V_{\min}$. In particular at the transitions, $\Delta V_i=V_i-V_{\min}$, where $i=0$, 1 or 2.

The voltages relative to $V_{\min}$ at the transitions described above are plotted as a function of current in Fig. 4 and as a function of concentration in Fig. 5. Figure 4 shows ΔV_0, ΔV_1, and $\Delta V_{\max}$ as a function of current for a set of runs with $c_0=0.3$ mol/liter. The feature at $(t_2,\Delta V_2)$ was very weak or absent in this set of runs. The error bars shown in Fig. 4 are based on estimates of the uncertainty in the measured transition times, and are as large as they are because V

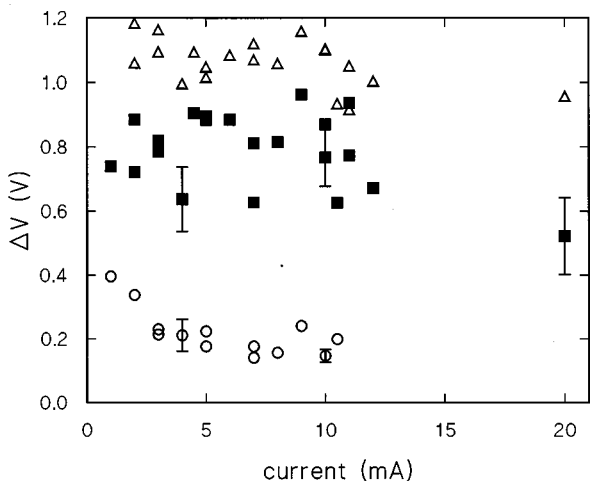

FIG. 4. The changes in cell voltage ΔV_0 (circles), ΔV_1 (squares), and $\Delta V_{\max}$ (triangles) at times t_0, t_1, and at the maximum of $V(t)$ plotted as a function of current for a set of runs with $c_0=0.3$ mol/liter.

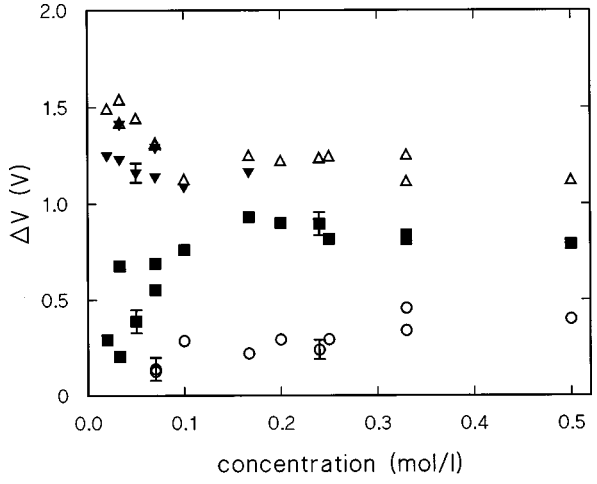

FIG. 5. The changes in cell voltage ΔV_0 (circles), ΔV_1 (squares), ΔV_2 (downward-pointing triangles), and $\Delta V_{\max}$ (upward-pointing triangles) at times t_0, t_1, t_2, and at the maximum of $V(t)$ plotted against concentration for a set of runs with $I=2.00$ mA.

is, by definition, changing rapidly at the transitions. For this set of runs the resistance of the electrolyte in the cell was approximately 1 kΩ, so the initial value of the Ohmic overpotential varied from 1 to 20 V as the current varied from 1 to 20 mA. In contrast, the values of the ΔV_i vary by only a few tenths of a volt over this range of currents. This indicates that the ΔV_i are not related to the voltage drop across the bulk of the electrolyte, but are rather due to other processes, which are approximately the same for all runs. The transition voltages ΔV_0, ΔV_1, and ΔV_2 are plotted along with $\Delta V_{\max}$ for a series of runs at $I=2.00$ mA in Fig. 5. The peak at t_0 is absent at low c_0, while at high c_0 that at t_2 is not observed. Figure 2, for $c_0=0.07$, is near the lower limit at which t_0 is visible. As above, the cell voltage varies by a factor of 20 over this range of concentrations, but the changes in the ΔV_i are much smaller.

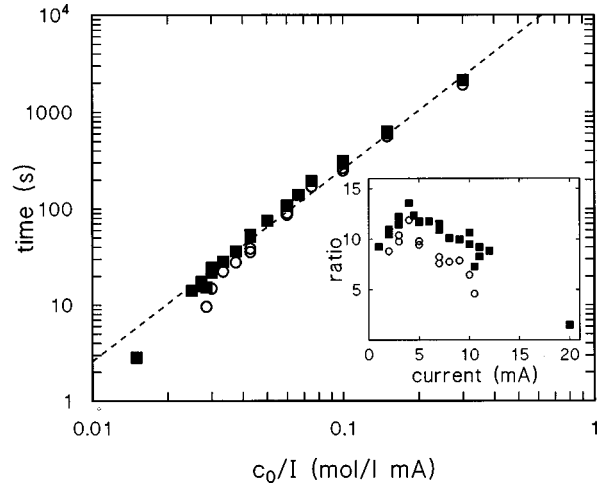

FIG. 6. The transition times t_0 (circles) and t_1 (squares) as a function of c_0/I for the same set of runs as in Fig. 4. The uncertainties in the data are approximately the size of the symbols, and the dashed line is a fit of the t_1 data to a square-law dependence on c_0/I. The inset shows the ratios of t_0 and t_1 to the Sand's time t_s for the same data, where t_s was calculated from Eq. (2) as discussed in the text.

TABLE I. Cell voltages ΔV_i (relative to $V_{\min}$) and corresponding standard electrode potentials $V^{\ominus}$ for the transitions at t_0 and t_1, and for the maximum in $V(t)$. The ΔV_i vary slightly with current and concentration as shown in Figs. 4 and 5; the data given here are representative values for $c=0.3$ mol/liter and $I=5$ mA. The data labeled $V^{\ominus}_{\rm ref}$ are standard electrochemical potentials of reactions discussed in the text.

	ΔV (V)	$V^{\ominus}$ (V)	$V^{\ominus}_{\rm ref}$ (V)
t_0	0.18 ± 0.04	0.16 ± 0.04	0.158
t_1	0.79 ± 0.12	-0.45 ± 0.12	
Max	1.08 ± 0.07	-0.74 ± 0.07	-0.828

The value of $\Delta V_{\max}$ plotted in Fig. 4 decreases slightly with increasing current. A straight-line fit to the data gives $\Delta V_{\max}=(1.12\pm0.03)-(0.009\pm0.003)I$, with ΔV measured in volts and I in mA. At $I=2.00$ mA, $\Delta V_{\max}$ decreases as c_0 increases for low concentrations, but becomes approximately constant at higher c_0. The average value of $\Delta V_{\max}$ for $c_0>0.15$ mol/liter is 1.20 ± 0.06 V, consistent with the low-current value determined from Fig. 4 at $c_0=0.3$ mol/liter. ΔV_0 decreases as I increases for low currents, then levels out; its average value for $I\geqslant5$ mA is 0.18 ± 0.04 V. At fixed current, ΔV_0 increases slightly with increasing c_0, and a linear fit to the data plotted in Fig. 5 gives $\Delta V_0=(0.14\pm0.04)+(0.64\pm0.15)c_0$, where c_0 is in units of mol/liter. The data for ΔV_1 shown in Fig. 4 do not vary systematically with current and have an average value of 0.79 ± 0.12 V. At lower concentrations, however, ΔV_1 decreases with increasing I. As a function of concentration, ΔV_1 increases roughly linearly at low c_0, and then flattens out. The average value of ΔV_1 for $c_0>0.15$ mol/liter is 0.85 ± 0.05 V. ΔV_2 decreases with increasing c_0 but shows no systematic variation with I over the range of concentration and current in which it was observed. Representative values of ΔV_0, ΔV_1, and $\Delta V_{\max}$ corresponding to $c_0=0.3$ mol/liter and $I=5$ mA are shown in Table I.

Figure 6 is a log-log plot of the transition times t_0 and t_1 for the same data as in Fig. 4, plotted as a function of c_0/I. A similar plot of t_0, t_1, and t_2 for the fixed current data of Fig. 5 is shown in Fig. 7. In both figures, the line is a fit of the t_1 data to the form $t_1=k(c_0/I)^2$. In all cases, t_0, t_1, and t_2 are approximately proportional to $(c_0/I)^2$, as predicted by Eq. (2) for the Sand's time. Figure 8 is a plot of t_1 against c_0/I for all runs, at a variety of concentrations and currents. The data collapse reasonably well onto a single line, indicating power-law behavior with an exponent of 2.05 ± 0.05. If we identify t_1 with the time at which the concentration of Cu^{2+} at the cathode goes to zero, then we can use Eq. (2) and the fitted value of k to extract a value for the effective diffusion constant. This gives $D_{\rm eff}=(5.66\pm0.26)\times10^{-5}$ cm^2/s for the t_1 data of Fig. 6, and $D_{\rm eff}=(6.30\pm0.44)\times10^{-5}$ cm^2/s for the data of Fig. 7. These are an order of magnitude larger than the value of $D=5.6\times10^{-6}$ cm^2/s for 0.1 mol/liter $CuSO_4$ [40]; normally one would expect D to decrease with increasing concentration [41]. These results are consistent with those of Argoul *et al.* [18], who found that the presence of convection led to Sand-like behavior but with an enhanced diffusion constant, and the substantial difference between $D_{\rm eff}$ and D indicates that convection con-

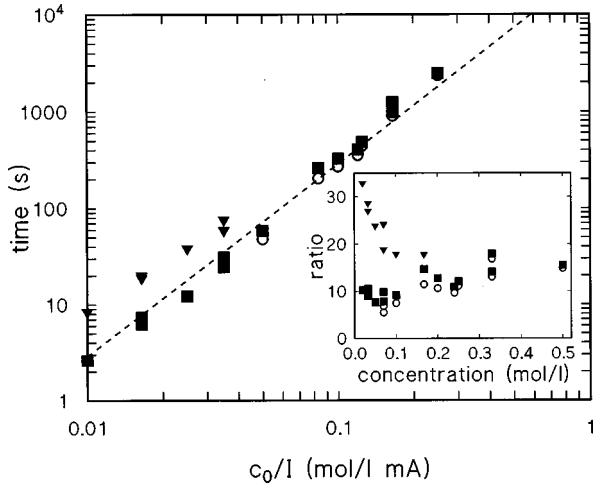

FIG. 7. The transition times t_0 (circles), t_1 (squares), and t_2 (triangles) as a function of c_0/I for the same set of runs as in Fig. 5. The dashed line is a fit of the t_1 data to a square-law dependence on c_0/I. The inset shows the ratios of t_0, t_1, and t_2 to t_s, where t_s was calculated from Eq. (2) as discussed in the text.

tributes substantially to the charge transport here.

Although Fig. 8 shows that on average t_1 is proportional to $(c_0/I)^2$, systematic deviations of the t_1 data from the fitted line can be seen in Figs. 6 and 7. These can be interpreted to mean that D_{eff} varies with current and concentration. This variation is illustrated in insets to Figs. 6 and 7, which show the ratios t_i/t_s for the same sets of runs. Here t_s is the Sand's time for purely diffusive transport, calculated from Eq. (2) using the above value of D for 0.1 mol/liter solutions.

The inset to Fig. 6 shows that the ratios for both t_0 and t_1 are of order 10. Both have a maximum around $I=4$ mA, and then decrease linearly for higher currents. The inset to Fig. 7 shows that both t_0/t_s and t_1/t_s increase linearly with increasing concentration, despite the fact that D itself should be decreasing with c_0. On the other hand, t_2/t_s is as high as 30 at low c_0, and decreases relatively rapidly with increasing

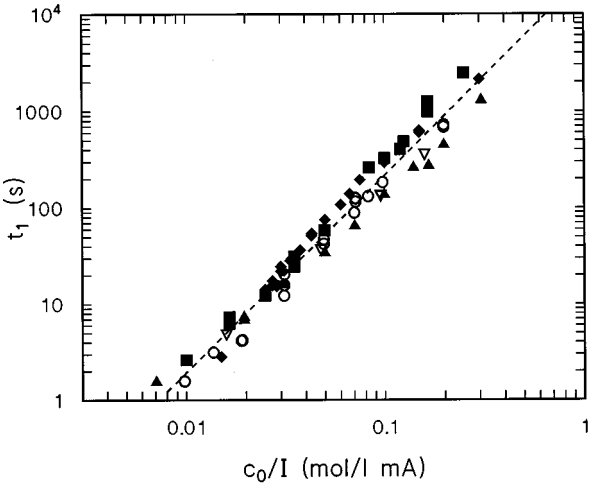

FIG. 8. The transition time t_1 vs c_0/I for all runs. Upward-pointing triangles: $c_0=0.02$ mol/liter; downward-pointing triangles: $c_0=0.05$ mol/liter; circles: $c_0=0.1$ mol/liter; diamonds: $c_0=0.3$ mol/liter; squares: $I=2.00$ mA. The dashed line is a fit of all of the data to a power law that gives an exponent of 2.05 ± 0.05.

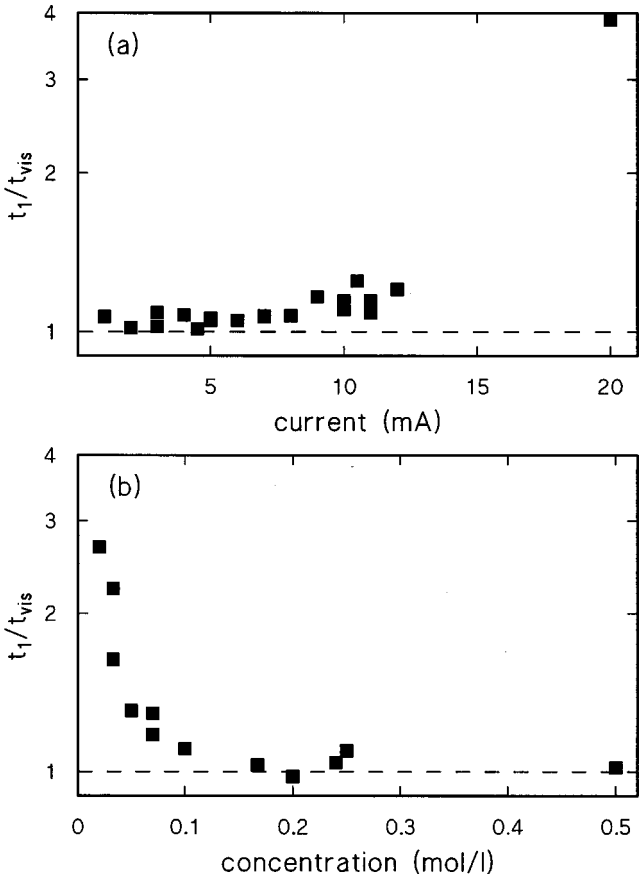

FIG. 9. (a) The ratio t_{vis}/t_1 for the t_1 data of Fig. 6. Note that the vertical axis is logarithmic. (b) The same ratio for the t_1 data of Fig. 7.

concentration in the range where that feature is observed.

t_1 is very close to the time at which rough growth is first visible with our imaging system. At a time t_{vis} roughness at the one-pixel level becomes visible on the cathode. Figure 9(a) shows the ratio t_{vis}/t_1 as a function of current for the data of Fig. 4, while Fig. 9(b) shows the same ratio as a function of concentration for the runs of Fig. 5. This ratio is close to but a few percent larger than one for $I\lesssim 5$ mA and for $c_0\gtrsim 0.15$ mol/liter, but increases for high current and low concentration, which are the conditions under which buoyancy-driven convection is expected to be less important. The fact that t_{vis}/t_1 is close to one over most of the parameter space studied here suggests that the transition at t_1 is associated with the onset of a morphological instability of the deposit growing on the cathode, and so with the onset of rough growth. That t_{vis} is always greater than t_1 can be accounted for by the limited resolution of the imaging system, since it takes time for the roughness to grow large enough to be seen.

The cell voltage can be calculated for the case of purely diffusive charge transport. The concentration $c(x,t)$ is determined using Eq. (1), and the cell voltage calculated as

$$V(t)=I\int_0^d \frac{dx}{\sigma}, \tag{4}$$

where d is the length of the cell. The conductivity σ is a

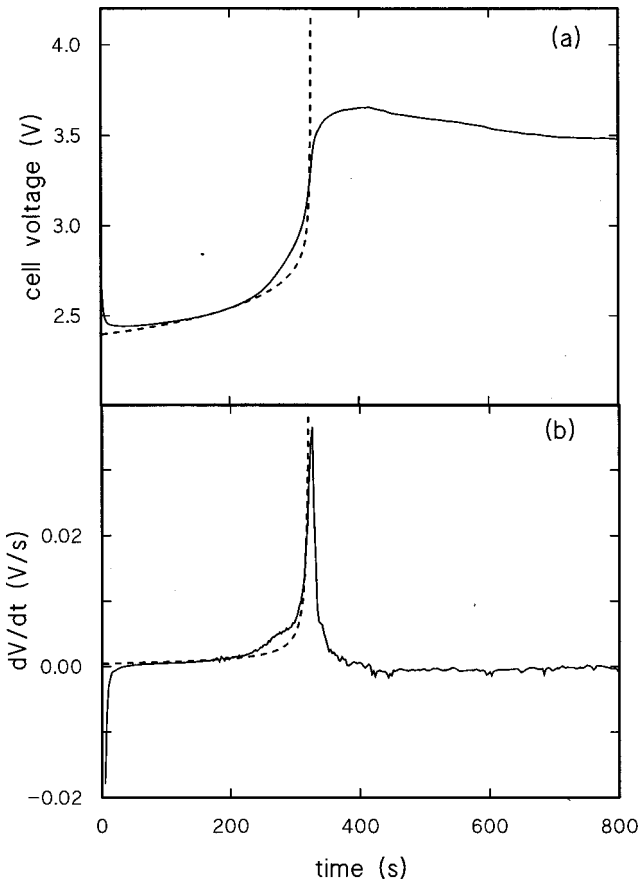

FIG. 10. The cell voltage (a) and dV/dt (b) for $c_0=0.2$ mol/liter and $I=2.00$ mA. The solid lines show the experimental data and the dashed lines are the corresponding quantities calculated from Eq. (4), assuming purely diffusive transport.

function of concentration and so of position x [37]. Figure 10(a) shows measured data for a run with $c_0=0.2$ mol/liter and $I=2.00$ mA, along with the voltage calculated from Eqs. (1) and (4). The corresponding values of dV/dt are plotted in Fig. 10(b). A value of $D_{\rm eff}=7.15\times10^{-5}$ cm^2/s, again much larger than the expected value, was used in the calculation to give a Sand's time for the calculation in agreement with the value of $t_1=327$ s measured for this run. The calculated voltage has been shifted downwards by 0.4 V to make it overlap with the measured data. Although there is fair qualitative agreement between the measurements and the calculated voltage, there are features in the data that do not appear in the calculated results. In particular, the initial transient drop in V, which accounts for at least part of the 0.4 V shift in $V(t)$ mentioned above, is discussed in Sec. III C below, while the shoulder that appears in both $V(t)$ and dV/dt prior to the main transition is the t_0 feature.

C. Initial transient

When the current through the cell is turned on at time $t=0$, the cell voltage very quickly rises to an initial value. It then decays over a time of order 10 s to a value a few tenths of a volt lower. This initial transient is visible in Figs. 2 and 10, and is shown in more detail in Fig. 11, which is a plot of $\Delta V(t)$ for the first 80 s of a run with $c_0=0.33$ mol/liter and $I=2.00$ mA. This transient was ascribed by Argoul *et al.*

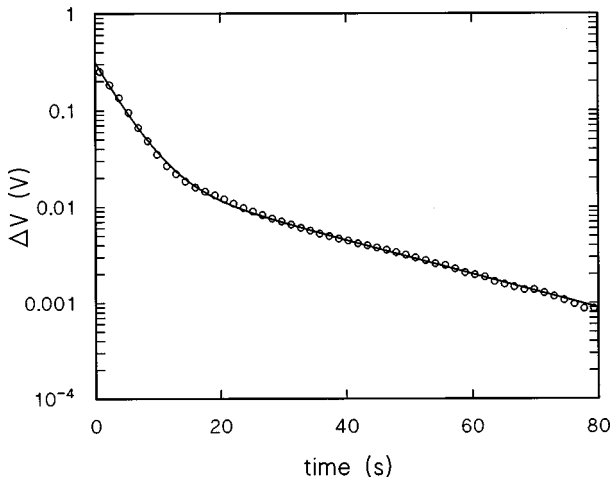

FIG. 11. The early-time decay of the cell voltage for a run with $c_0=0.33$ mol/liter and $I=2.00$ mA. For this run the data, shown as circles, are well described by a fit to the sum of two decaying exponentials, shown as a solid line.

[18] to double layer charging damped by the onset of buoyancy-driven convection, while Rosso *et al.* [20] referred to the initial overshoot as a ''nucleation peak.'' Charging of the double layer will indeed occur when the cell current is turned on, as discussed in the Introduction. However, it would result in a rounding of the voltage-time curve as the voltage *increased* to a final value, exactly analogous to the charging of a capacitor. Since the capacitance of the double layer is typically 20 μF/cm^2, the cross-sectional area of the experimental cell was 0.125 cm^2, and the resistance of the electrolyte (which depended on c_0) was on the order of a few kΩ, the RC time constant of the double layers with no aggregate present was on the order of a few milliseconds. Thus this process is very fast on the time scale of Fig. 11, and most likely does not contribute significantly to the transient plotted there.

The transients for all runs were fitted to a single decaying exponential of the form $V_b+\alpha e^{-\beta t}$, and to the sum of two exponentials, $V_b+\alpha e^{-\beta t}+\gamma e^{-\delta t}$. The decay constants β and δ, the amplitudes α and γ, and the background voltage V_b were used as fitting parameters. At low concentrations and high currents the transient was well described by a single exponential decay, while at high concentrations and low currents, as in Fig. 11, it was best described by the sum of two decaying exponentials. Figure 12(a) shows the time constants (i.e., the reciprocals of the decay constants β and δ) determined from these fits as a function of concentration for a series of runs with $I=2.00$ mA. The corresponding amplitudes α and γ are plotted in Fig. 12(b). In all cases the statistical uncertainties in the fit parameters are roughly the size of the plotted symbols, and significantly smaller than the scatter in the results. At this current, there is a transition from one-exponential to two-exponential decay between $c_0=0.07$ and 0.1 mol/liter. Results from a number of concentrations and currents are plotted in Fig. 13. The transient is a single exponential decay above a line given by $I=(18.6\pm1.5)c_0$, and the sum of two exponentials below that line.

The time constants and amplitudes of the single-exponential decay appear to be the same as those of the faster of the two decays observed in the two-exponential re-

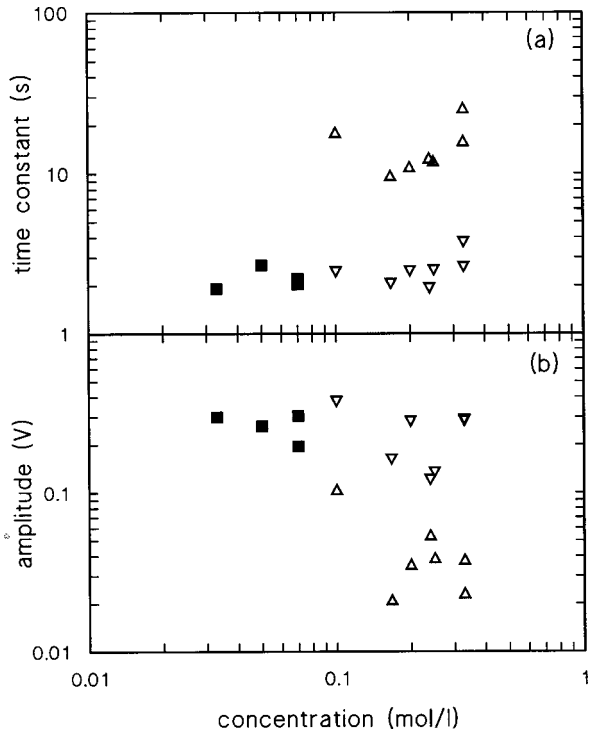

FIG. 12. (a) Time constants and (b) amplitudes from fits to the initial transient decay of $V(t)$, for a series of runs at $I=2.00$ mA. The solid squares are the results of fits to a single exponential decay, while the open triangles are the results of fits to the sum of two exponentials. Upward-pointing triangles correspond to the slow process and downward-pointing triangles to the fast process discussed in the text. Statistical uncertainties in the fit parameters are approximately the size of the symbols.

gion. The time constant for this process is about 2 s, is independent of concentration within the experimental scatter, and decreases with increasing current. There is considerable scatter in the results for the amplitudes, but no systematic variation was observed as a function of either concentration or current. The slower process, on the other hand, has a time constant of 10–20 s, increasing with increasing concentration and decreasing with increasing current.

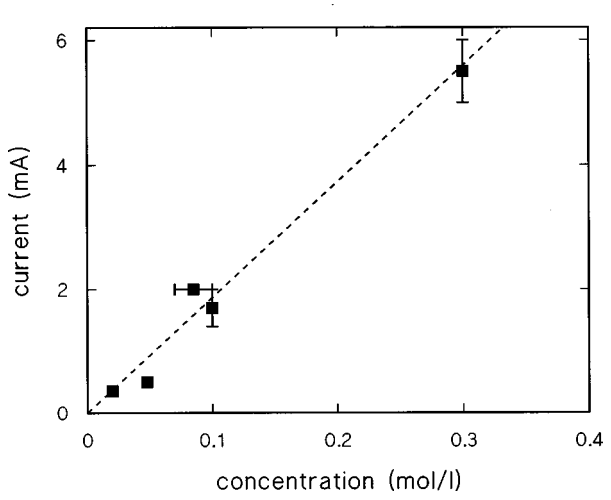

FIG. 13. Diagram showing the boundary between the regions in which the transient was described by a single- and a two-exponential decay. The transient was a single exponential decay above the dashed line, which is a fit through the origin to the plotted points.

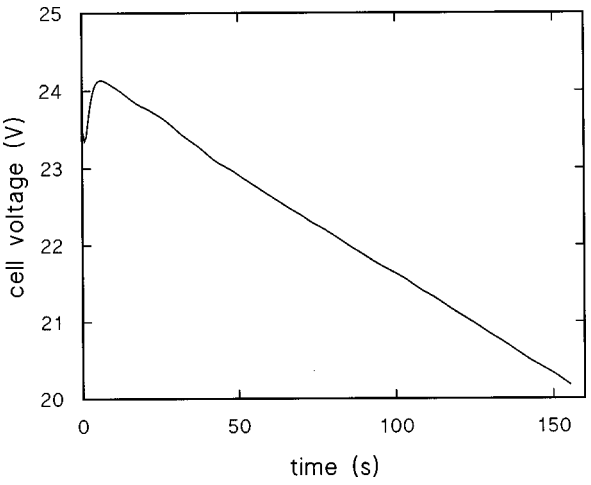

FIG. 14. $V(t)$ for a run with $c_0=0.1$ mol/liter and $I=10.21$ mA. Note the linear decrease in cell voltage after the peak.

Thus there appear to be two processes involved in the transient. At least one may be connected with the development of buoyancy-driven convection near the electrodes. This will occur for all concentrations, but will be stronger for larger c_0. The characteristic time scale for buoyancy-driven flows is $\tau=\pi d/4v_{\max}$ where $v_{\max}$ is the maximum convective flow velocity. Huth *et al.* [23] found this time to be about 6 s in a cell 0.25 mm thick, the same thickness as used in the present experiments. The data in their paper [23] show that buoyancy-driven convection rolls are fully established near the electrodes 15 s into an experiment, for experimental parameters comparable to those used in this work. It thus seems reasonable to associate the slower exponential relaxation, which becomes important at high concentrations and low currents, with the development of convective flows near the electrodes.

D. Falloff at longer times

Equation (3) indicates that $V(t)$ should decrease linearly with time once the aggregate starts growing on the cathode. This is the case in Fig. 2 for $t\gtrsim 200$ s, but the linear falloff is more obvious in Fig. 14, for which $c_0=0.1$ mol/liter and $I=10.2$ mA. Figure 15 shows the average slope m of the linear decrease plotted against I^2 for two sets of experiments at two different concentrations. We find $m\propto I^2$ as expected, with the constant of proportionality dependent on concentration. Using Eq. (3), the effective anion mobility $\mu_{\rm eff}$ can be calculated from the slopes of lines fitted to data like that in Fig. 15. The results are plotted as a function of c_0 in the inset to Fig. 15. The values obtained for the three highest concentrations are equal within experimental uncertainties; their average value is $(2.34\pm 0.04)\times 10^{-4}$ cm^2/V s. As expected [41], and as noted previously [11], this is lower than the tabulated value of 8.29×10^{-4} cm^2/V s for the mobility of the SO_4^{2-} ion at zero concentration.

The linear decrease in $V(t)$ is due to a linear increase in length of the growing aggregate. However, the decrease in $V(t)$ is not perfectly linear, nor does the aggregate grow

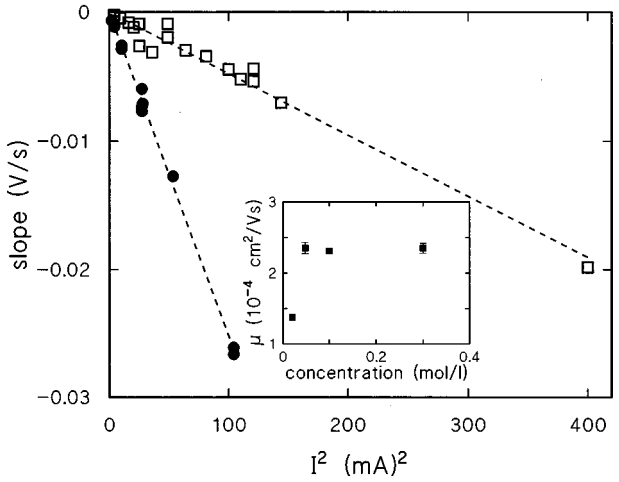

FIG. 15. The slope of $V(t)$ in the regime of linear decrease plotted as a function of I^2, for runs with $c_0 = 0.1$ mol/liter (circles) and $c_0 = 0.3$ mol/liter (squares). The dashed lines are linear fits to the data. The inset shows the anion mobility μ determined from the slopes of the fitted lines, as a function of concentration.

uniformly or at a perfectly constant speed. If the front of the aggregate advances more quickly than average, then $V(t)$ will decrease more quickly, while if the front advances more slowly, V will decrease less quickly. Such detailed features of the growth lead to fluctuations in $V(t)$, or correspondingly in dV/dt. The cell voltage is an average measure of what is happening within the cell, rather than a probe of local growth phenomena, so morphological features on a particular branch, such as a major branching event or even a stoppage of the growth of that tree, will not necessarily give a strong signature in the cell voltage. Rather, the contribution of such events to $V(t)$ will tend to be smeared out by contributions due to all of the other trees. Nonetheless, in some cases it is possible to link certain events in the growth of the aggregate with features in the $V(t)$ data.

Figure 16(a) shows a composite image of the aggregate grown in a run with $c_0 = 0.033$ mol/liter and $I = 2.00$ mA. A series of 5 images taken at different times have been subtracted and the result thresholded to indicate the growth that occurred during each time interval. The horizontal field of view in this image is 9.1 mm, corresponding to 36% of the entire cell. Note that the image processing used in this case has resulted in the loss of much of the fine detail visible in the original video images. Figure 16(b) shows the corresponding voltage plot. Figure 16(a) indicates that an initial period of uniform growth was followed by the appearance of rough growth. At $t \approx 40$ s, a large number of trees stopped growing. This event is accompanied by a small plateau in $V(t)$. For a period around $t = 150$ s, $V(t)$ decreases more steeply than average. Around this time, two of the trees shown in Fig. 16(a) stop growing, but there are also major branching events on two of the surviving trees. Since a steeper decrease in $V(t)$ implies faster growth on average, it appears that the branching contributes more to $V(t)$ in this particular case. Similarly around $t = 220$ s, the formation of major branches on some trees is accompanied by a faster decrease in $V(t)$. On the other hand, the steepening in $V(t)$ which occurs around $t = 315$ s does not seem to be associated with any particular morphological feature visible in Fig.

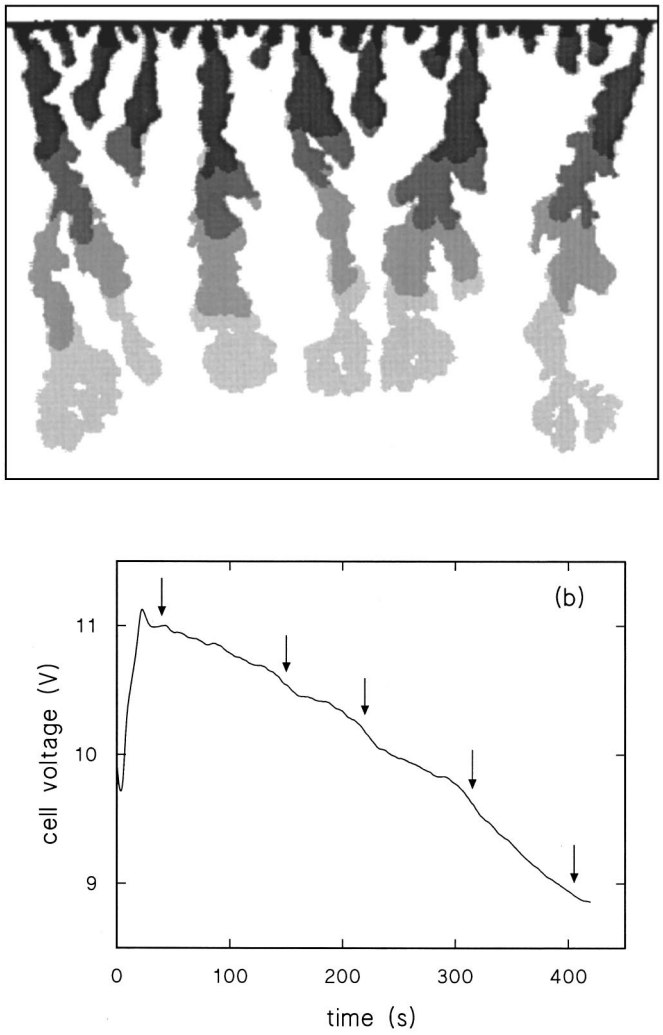

FIG. 16. (a) A composite image of the aggregate grown in a run with $c_0 = 0.033$ mol/liter and $I = 2.00$ mA. Starting with the darkest shade, the different shadings indicate the portion of the aggregate, which was deposited during the time intervals 0–40 s, 40–150 s, 150–220 s, 220–315 s, and 315–405 s. (b) $V(t)$ for the same run. The arrows indicate the times at which the subimages in (a) were recorded.

16(a), although of course other things could have occurred in regions of the cell not shown in the figure. A sudden increase in the rate and quantity of branching on the trees (the Hecker transition [10,16]) occurs throughout the cell at $t \approx 360$ s. There is no obvious sign of this transition in the voltage curve, despite the fact that it is visually quite obvious.

It seems clear that the structure in the voltage data in this regime is due to the details of the growth process taking place in the cell. However, because the voltage is an averaged quantity, it is difficult to draw any detailed correspondence between the morphological features and the features in the $V(t)$ data except in a few extreme cases.

IV. DISCUSSION

The transitions observed in the cell voltage indicate changes in the electrode processes. To get some understanding of what happens at the three transitions seen in this work, it is useful to convert our values of ΔV into standard elec-

trochemical potentials. Standard electrochemical potentials are defined relative to that for the reaction $2H^+ + 2e^- \rightarrow H_2$ at a standard hydrogen electrode, which is assigned a potential of 0 V. We denote the standard electrochemical potential of our cathode by the symbol $V^{\ominus}$. Since we did not measure potentials relative to a reference electrode, we make the assumptions that, at the start of a run, the electrochemical reaction at the cathode is $Cu^{2+} + 2e^- \rightarrow Cu$, and that $V^{\ominus}$ is equal to 0.340 V, the standard electrochemical potential for this reaction, when the cell voltage is equal to $V_{\min}$. Given the former assumption, the potential errors introduced by the latter are approximately the same size as the scatter in the data for the transition voltages plotted in Figs. 4 and 5. The standard electrochemical potential of the cathode is then given by $V^{\ominus} = 0.340\text{V} - \Delta V$. Representative values of $V^{\ominus}$ corresponding to the transitions and to $V_{\max}$ are shown in Table I.

The values of $V^{\ominus}$ in Table I can be compared to the electrochemical potentials for other reactions. The standard electrochemical potential for the reaction $Cu^{2+} + e^- \rightarrow Cu^+$ is $V^{\ominus} = 0.158$, close to the observed value of $V^{\ominus}$ at t_0. That for the electrolysis of water, $2H_2O + 2e^- \rightarrow H_2 + 2OH^-$, is $V^{\ominus} = -0.828$ V, which is close to the values of $V^{\ominus}$ at both t_2 and at $V_{\max}$. The electrochemical potentials for these reactions are listed in Table I as $V^{\ominus}_{\text{ref}}$. The correspondence between these values and the measured electrochemical potentials suggests that the changes in $V(t)$ that occur at these times may be associated with the onset of these electrochemical reactions. There is no obvious candidate reaction with $V^{\ominus}$ in the near neighborhood of the value observed at t_1, but as discussed above this transition is associated with a *physical* change in the nature of the electrode, namely, the morphological instability of the growing aggregate, rather than a change in the electrochemistry. This instability is triggered by the depletion of copper ions at the cathode and leads to the appearance of rough growth on the electrode. Popov *et al.* [42] measured the critical overpotential for the formation of rough copper deposits to be 0.66 V, which is slightly lower than the average values of ΔV_1, but not inconsistent with the data of Figs. 4 and 5. The nature of the transitions is not completely straightforward, however, since the transition voltages vary somewhat with current and concentration.

It is apparent that much of the data presented in Sec. III are strongly affected by the presence of convection. Convection will be relatively important at low currents, when the contributions to the charge transport due to migration and diffusion are smaller, and at high concentration, when the convective flows are themselves strongest.

The effects of convection are perhaps most obvious in the case of the transition times, and particularly t_1. On average t_1 is proportional to $(c/I)^2$ as predicted by Eq. (2). However the ratio of t_1 to the Sand's time t_s calculated assuming purely diffusive transport is approximately 10, and t_1/t_s tends to increase as concentration increases and current decreases, i.e., as convection becomes more important. t_1/t_s is equal to D_{eff}/D, so this indicates that the transport of ions to the cathode is substantially enhanced over what is expected for a purely diffusive system, and that convection delays by a factor of 10 the depletion of Cu^{2+} ions there. This has also been observed by others [18,20], and is consistent with the theoretical result of Chazalviel *et al.* [15] that the combination of diffusion and convection is described by a nonlinear diffusion equation with an enhanced diffusion constant.

The peak in dV/dt at time t_0 is strongest at high concentration and low current, and so this transition appears to be enhanced by convection. One possible scenario consistent with the electrode voltages determined above is that the flux of Cu^{2+} ions arriving at the cathode is enhanced by convection to the point that not all of the ions can be reduced to metallic copper at the imposed constant current, and so some or all of them are only partially reduced to Cu^+. This transition and the oscillations associated with it will be the subject of future work. The transition at t_2 is quite different, in that the ratio t_2/t_s decreases as concentration increases, and the feature is not observed at high concentrations and high currents.

At t_1, the concentration of ions goes to zero at the cathode and the metal aggregate being deposited there becomes unstable. At high concentrations and low currents, i.e., when convection is most significant, the time at which roughness becomes visible with our imaging system is essentially the same as t_1. However, when convection is expected to be weaker, roughness is not visible on the cathode until three or four times t_1. This suggests that convective transport enhances the growth rate of the instability, consistent with the results of Ref. [34], in which the growth rate of the instability at the cathode was found to be substantially larger than that predicted theoretically assuming purely diffusive transport [32].

As discussed above, the transient drop in the cell voltage immediately after the current is applied appears to be due at least in part to convection, since the slower of the two relaxation processes that contribute to the transient is observed in the regime where convection is expected to be important, and has a time scale approximately equal to that characterizing the convective flow. The other process is faster and occurs at all currents and concentrations; its nature is unclear. One process considered as a possibility was Ohmic heating of the electrolyte, which would cause an increase in the electrolyte conductivity and thus a decrease in the cell voltage. However, the amount of power dissipated in the electrolyte, which is of the order of a few mW, is only enough to account for a few percent of the observed voltage decrease.

The long-time decrease of $V(t)$ is approximately linear, with the average slope proportional to I^2 as predicted by Eq. (3) [11]. The values of the anion mobility determined from dV/dt in this regime are smaller than the tabulated value for zero concentration, as expected [41]. Fluctuations in dV/dt in this regime are due to local details of the growth of the branched aggregate, with local growth spurts tending to make $V(t)$ decrease more quickly, and stagnating branches leading to a slower decrease. However, except in extreme cases it is difficult to convincingly link every wiggle in $V(t)$ with a particular morphological feature, since the cell voltage involves an average over all parts of the aggregate.

V. CONCLUSIONS

A very general conclusion that can be drawn from this work is that buoyancy-driven convection has a strong influence on this system, particularly at early times before the

appearance of rough growth, and during the initial development of the instability of the cathode, which leads to rough growth. Convection delays the onset of the instability by an order of magnitude in time, but also enhances the growth of the rough aggregate once the instability occurs. The influence of convection is stronger at high concentrations and low currents.

The rapid increase in $V(t)$ before it peaks and then starts to decrease is due to a sequence of transitions in the cathode processes, including the morphological instability of the cathode itself at t_1. The transition at t_0, prior to the instability, appears to be enhanced by convection and is associated with oscillations in the cell voltage. It may thus involve oscillations in the electrochemical reactions taking place at the cathode, perhaps including the reduction of Cu^{2+} to Cu^{+} rather than to metallic copper. The transition at t_2, after the instability, and the location of the peak in $V(t)$, may be associated with the onset of water electrolysis.

As the branched aggregate develops, it grows approximately linearly in time [9,22], and so the cell voltage decreases linearly with time. Fluctuations in $V(t)$ in this regime are caused by local variations in the growth rate of individual branches of the aggregate.

This work was aimed at developing some understanding of the interplay among the many processes involved in ECD in thin layers through a detailed study of the cell voltage. Both electrochemical and physical phenomena contribute to the complicated time dependence of $V(t)$. A more detailed study of the voltage oscillations observed both before and after the instability of the cathode that occurs at the main transition would be of interest, as would a more quantitative examination of the electrochemical reactions associated with the transitions.

ACKNOWLEDGMENTS

This research was supported by the Natural Sciences and Engineering Research Council of Canada, and in part by the Office of the Dean of Science, Memorial University of Newfoundland. I am grateful to G. Marshall, G. White, F. Smith, and S. Morris for helpful discussions.

[1] E. Ben-Jacob and P. Garik, Nature (London) **343**, 523 (1990).
[2] T. Viscek, *Fractal Growth Phenomena* (World Scientific, Singapore, 1992).
[3] Y. Sawada, A. Dougherty, and J. P. Gollub, Phys. Rev. Lett. **56**, 1260 (1986).
[4] D. Grier, E. Ben-Jacob, R. Clarke, and L. M. Sander, Phys. Rev. Lett. **56**, 1264 (1986).
[5] P. P. Trigueros, J. Claret, F. Mas, and F. Sagués, J. Electroanal. Chem. **312**, 219 (1991).
[6] D. Barkey, F. Oberholtzer, and Q. Wu, Phys. Rev. Lett. **75**, 2980 (1995).
[7] F. Argoul, A. Arneodo, G. Grasseau, and H. L. Swinney, Phys. Rev. Lett. **61**, 2558 (1988).
[8] J.-N. Chazalviel, Phys. Rev. A **42**, 7355 (1990).
[9] V. Fleury, J.-N. Chazalviel, M. Rosso, and B. Sapoval, J. Electroanal. Chem. **290**, 249 (1990).
[10] V. Fleury, M. Rosso, and J.-N. Chazalviel, Phys. Rev. A **43**, 6908 (1991).
[11] V. Fleury, M. Rosso, J.-N. Chazalviel, and B. Sapoval, Phys. Rev. A **44**, 6693 (1991).
[12] V. Fleury, J.-N. Chazalviel, and M. Rosso, Phys. Rev. Lett. **68**, 2492 (1992).
[13] V. Fleury, J.-N. Chazalviel, and M. Rosso, Phys. Rev. E **48**, 1279 (1993).
[14] V. Fleury, J. Kaufman, and B. Hibbert, Phys. Rev. E **48**, 3831 (1993).
[15] J.-N. Chazalviel, M. Rosso, E. Chassaing, and V. Fleury, J. Electroanal. Chem. **407**, 61 (1996).
[16] A. Kuhn and F. Argoul, Phys. Rev. E **49**, 4298 (1994); J. Electroanal. Chem. **371**, 93 (1994).
[17] F. Argoul and A. Kuhn, Physica A **213**, 209 (1995).
[18] F. Argoul, E. Freysz, A. Kuhn, C. Léger, and L. Potin, Phys. Rev. E **53**, 1777 (1996).
[19] D. P. Barkey, D. Watt, Z. Liu, and S. Raber, J. Electrochem. Soc. **141**, 1206 (1994).
[20] M. Rosso, J.-N. Chazalviel, V. Fleury, and E. Chassaing, Electrochim. Acta **39**, 507 (1994).
[21] C. Livermore and P.-z. Wong, Phys. Rev. Lett. **72**, 3847 (1994).
[22] K. Linehan and J. R. de Bruyn, Can. J. Phys. **73**, 177 (1995).
[23] J. M. Huth, H. L. Swinney, W. D. McCormick, A. Kuhn, and F. Argoul, Phys. Rev. E **51**, 3444 (1995).
[24] D. Barkey, J. Electrochem. Soc. **138**, 2912 (1991).
[25] R. M. Suter and P.-z. Wong, Phys. Rev. B **39**, 4536 (1989).
[26] F. Argoul, J. Huth, P. Merzeau, A. Arneodo, and H. L. Swinney, Physica D **62**, 170 (1993).
[27] F. Argoul and A. Kuhn, J. Electroanal. Chem. **359**, 81 (1993).
[28] E. Chassaing, M. Rosso, B. Sapoval, and J.-N. Chazalviel, Electrochim. Acta **38**, 1941 (1993).
[29] The concentration gradients that develop at both electrodes lead to voltages known as concentration overpotentials. The cathodic concentration overpotential makes the cathode more negative with respect to the anode, i.e., it makes the cell voltage larger. At the anode, on the other hand, the concentration overpotential makes the cell voltage smaller. This is one anodic phenomenon that is known to contribute to the total cell voltage, however, its magnitude is small, being given by $\eta = RT\ln(c_e/c_0)/nF$. Here R is the gas constant, T the temperature, n the number of electrons transferred by the electrode reaction, F the Faraday constant, and c_e the concentration near the electrode. Even if the concentration at the anode was 10 times larger than in the bulk, the overpotential η would only be 0.03 V.
[30] D. D. MacDonald, *Transient Techniques in Electrochemistry* (Plenum, New York, 1977).
[31] W. W. Mullins and R. F. Sekerka, J. Appl. Phys. **34**, 323 (1963); **35**, 444 (1964).
[32] D. P. Barkey, R. H. Muller, and C. W. Tobias, J. Electrochem. Soc. **136**, 2207 (1989).
[33] M. D. Pritzker and T. Z. Fahidy, Electrochim. Acta **37**, 103 (1992).

[34] J. R. de Bruyn, Phys. Rev. E **53**, R5561 (1996).
[35] G. Marshall and P. Mocskos, Phys. Rev. E **55**, 549 (1997).
[36] V. Fleury, J. H. Kaufman, and D. B. Hibbert, Nature (London) **367**, 435 (1994).
[37] The conductivity data tabulated in [38] were well described by the empirical fitting function $\sigma = -0.10350c_0 + 0.14501c_0^{0.9046}$ for $0 \leqslant c_0 \leqslant 0.5$ mol/liter.
[38] *Handbook of Chemistry and Physics*, 52nd ed. edited by R.C. Weast (Chemical Rubber Company, Cleveland, 1971).
[39] Fisher Certified anhydrous $CuSO_4$, minimum purity 97%. Dissolved oxygen and small amounts of other chemical impurities have been shown to have a significant effect on the growth and morphology of the deposited aggregate [16]. However, since the main interest in the present work centered on early times, when the growth is just getting started, and not on the actual morphology of the aggregate, no attempt was made to further purify the electrolyte; in particular dissolved oxygen was not removed from the solution by bubbling nitrogen gas through it.
[40] J. S. Newman, *Electrochemical Systems* (Prentice-Hall, Englewood Cliffs, NJ, 1973).
[41] A. L. Horvath, *Handbook of Aqueous Electrolyte Solutions* (Ellis Horwood, Chichester, 1985).
[42] K. I. Popov, M. D. Maksimovic, J. D. Trnjancev, and M. G. Pavlovic, J. Appl. Electrochem. **11**, 239 (1981).